

# $\gamma$ -Al<sub>2</sub>O<sub>3</sub> 柔性纳米纤维膜的制备及机械性能

李 微<sup>1</sup>, 赵晓敏<sup>2</sup>, 王延凤<sup>3</sup>, 路文娟<sup>3</sup>, 贾玉娜<sup>1,4</sup>, 焦秀玲<sup>1,4</sup>, 陈代荣<sup>1,4</sup>, 张平平<sup>3</sup>

(1. 山东大学化学与化工学院, 济南 250100; 2. 山东大学生命科学学院, 济南 250100;

3. 山东省医学科学院药物研究所, 济南 250062; 4. 国家胶体材料工程技术研究中心, 济南 250100)

**摘要** 以氯化铝和异丙醇铝为原料, 水和乙醇为溶剂, 通过溶胶凝胶结合静电纺丝法制备了柔性  $\gamma$ -Al<sub>2</sub>O<sub>3</sub> 纳米纤维膜. 表征了纤维膜的形貌和机械性质, 并研究了纤维膜的形成过程. 组成纤维膜的纤维直径均匀, 平均直径 188 nm, 纤维由粒径在 15~30 nm 的纳米颗粒组成且表面光滑. 制备的纤维膜具有较好的柔性及抗拉强度(1.01 MPa).

**关键词** Al<sub>2</sub>O<sub>3</sub>; 纤维膜; 机械性质; 静电纺丝

中图分类号 O614 文献标志码 A

## Fabrication and Mechanical Properties of Flexible $\gamma$ -Al<sub>2</sub>O<sub>3</sub> Nanofibrous Membranes

LI Wei<sup>1</sup>, ZHAO Xiaomin<sup>2</sup>, WANG Yanfeng<sup>3</sup>, LU Wenjuan<sup>3</sup>, JIA Yuna<sup>1,4</sup>,  
JIAO Xiuling<sup>1,4</sup>, CHEN Dairong<sup>1,4</sup>, ZHANG Pingping<sup>3\*</sup>

(1. School of Chemistry & Chemical Engineering, Shandong University, Jinan 250100, China;

2. School of Life Sciences, Shandong University, Jinan 250100, China;

3. Institute of Materia Medica, Shandong Academy of Medical Sciences, Jinan 250062, China;

4. National Engineering Research Center for Colloidal Materials, Shandong University, Jinan 250100, China)

**Abstract** Flexible  $\gamma$ -Al<sub>2</sub>O<sub>3</sub> nanofibrous membranes were prepared by sol-gel combined electrospinning technique using aluminum chloride and aluminum isopropoxide as raw materials, water and ethanol as the solvents. The morphology and mechanical property of the membranes were characterized and the formation process was tracked. The membranes were composed of uniform nanofibers with a mean diameter of *ca.* 188 nm. The fibers' surfaces were smooth and the fibers were composed of nanoparticles with a size range of 15—30 nm. The prepared membranes exhibited excellent flexibility and tensile strength(1.01 MPa).

**Keywords** Al<sub>2</sub>O<sub>3</sub>; Fibrous membrane; Mechanical property; Electrospinning

As an important structural functional material, alumina has attracted great interest due to its high-melting point, low thermal conductivity, excellent thermo-stability, corrosion resistance, and chemical inertness to oxidizing and reducing atmospheres at high temperature<sup>[1,2]</sup>. Alumina fiber products have wide applications in multiple areas, including high temperature insulation<sup>[3]</sup>, filtration<sup>[4]</sup>, adsorption<sup>[5]</sup>, catalysts, and enhancement components for ceramics, metals and polymers. Normally, the fibers are brittle with a diameter in micron

收稿日期: 2016-11-29. 网络出版日期: 2017-05-22.

基金项目: 山东省医学科学院医药卫生科技创新工程、国家自然科学基金(批准号: 21305079)和山东省自然科学基金(批准号: ZR2015YL040)资助.

联系人简介: 张平平, 女, 博士, 助理研究员, 主要从事无机合成与材料化学研究. E-mail: pingpingzhang6087@163.com

scale and a length of several centimeters. In order to be more conveniently applied, the fibers are often made into two-dimensional objects such as fiber felt or blankets through post processing. However, the properties of the objects often suffer from the large diameters of the fibers, as well as the small surface area and large pore size.

Electrospinning is a remarkably simple and versatile technique that has been successfully used to prepare fibers of a broad range of organic polymers or inorganic ceramic oxides with a fiber diameter from tens of nanometers to hundreds of nanometers. Two-dimensional fiber mats such as nanowebs<sup>[6]</sup> and thin fibrous membranes<sup>[7]</sup> can be directly obtained by this method<sup>[8]</sup>. Electrospun fibrous membranes possess remarkable specific surface area, high porosity, an interconnected open pore structure, and high permeability<sup>[6,7]</sup> and have attracted much attention in sensor and separation fields. Many researchers prepared various kinds of membranes, including fluorinated polyurethane composite membranes<sup>[9]</sup> and polyacrylonitrile membranes<sup>[10]</sup>. However, the low thermal stability of the polymers prevents them from being used in high-temperature areas<sup>[7]</sup>. Considering inorganic membranes' high-temperature thermal stability, researchers have made considerable efforts to prepare inorganic membranes, such as SiO<sub>2</sub><sup>[7]</sup>, TiO<sub>2</sub><sup>[11]</sup>, and SiO<sub>2</sub>-TiO<sub>2</sub> composite membranes<sup>[12]</sup>. But their low strength and the high brittleness hinder their applications, and the preparation of flexible inorganic fibers mats with high strength still presents great challenges.

Generally, alumina fibers are brittle. According to previous reports, the mechanical properties of the alumina fibrous membrane depend on the fibers' diameter<sup>[13]</sup>, density<sup>[14]</sup>, the size of grains forming the fibers<sup>[13]</sup> and the fibers' geometric arrangement<sup>[15]</sup>. For example, more inter-fibrous fusions and higher crystallinity lead to a higher stiffness of membrane<sup>[16]</sup>. The fibers' flexibility can be promoted by decreasing their diameter and the size of the particles composing the fibers<sup>[13]</sup>. Therefore, it is very important to control the size of the particles, diameter, density, as well as the arrangement of the fibers in the membranes. In this study,  $\gamma$ -Al<sub>2</sub>O<sub>3</sub> fibrous membranes composed of independent interlaced thin fibers, which were composed of fine grains, were prepared *via* the electrospinning method. The prepared  $\gamma$ -Al<sub>2</sub>O<sub>3</sub> fibrous membranes exhibited excellent flexibility and high tensile strength.

## 1 Experimental

### 1.1 Materials

Aluminium isopropoxide (AIP, industrial grade, Jinan Taihua Chemical Industry Co., Ltd.); hydrochloric acid (HCl, A.R., 36%—38%, Laiyang Economic and Technological Development Zone Fine Chemical Factory); tartaric acid (C<sub>4</sub>H<sub>6</sub>O<sub>6</sub>, A. R.), aluminum chloride (AlCl<sub>3</sub> · H<sub>2</sub>O, A. R.), polyvinylpyrrolidone (PVP-K90,  $M_w = 1.3 \times 10^6$ ) and absolute ethyl alcohol (C<sub>2</sub>H<sub>5</sub>OH, A.R.) (Sinopharm Chemical Reagent Co., Ltd.). All the chemicals were used as received without further purification. The water used was deionized water with a resistance of 18.2 M $\Omega$ .

### 1.2 Preparation of Precursor Sol

In this experiment, 1.207 g of AlCl<sub>3</sub> · 6H<sub>2</sub>O was dissolved in 3.7 mL of water, followed by orderly additions of 2.553 g of AIP, 5 mL of ethyl alcohol, 0.143 g of tartaric acid and 1.7 mL of hydrochloric acid at room temperature with continuous magnetic stirring for 8 h. Then, 1.4% PVP (mass fraction) was added with vigorous stirring until the transparent spinnable precursor sol was formed.

### 1.3 Electrospinning of Membranes

The sol was transferred into a 10 mL syringe equipped with a metal spinneret which connected with a high-voltage generator. The gel fibrous membranes were spun at 20 kV, and the distance between the tip and metal grid collector was 20 cm. The feeding rate of the precursor solution was 1.9 mL/h. The membranes were spun at constant temperature (20 °C) and relative humidity (10%).

The obtained gel fibrous membranes were dried at 70 °C for 48 h to form xerogel fibrous membranes at first, and then calcined in air from room temperature to 600 °C with a rate of 2 °C/min and kept at 600 °C for 1.5 h, followed by being calcined to 800 °C with a rate of 10 °C/min and kept at 800 °C for 1.5 h to obtain  $\gamma$ - $\text{Al}_2\text{O}_3$  nanofibrous membranes. As a comparison, the nanofibrous membranes being calcined to 700 °C with the same calcination process were prepared.

#### 1.4 Characterization

Thermal behaviors of the fibrous membranes were studied by thermal gravimetric (TG) and differential scanning calorimetric (DSC) analyses (Mettler Toledo, TGA/SDTA851e) in air with a heating rate of 10 °C/min from room temperature to 900 °C. X-ray diffraction (XRD) patterns of the samples were characterized on a Rigaku D/Max 2200PC diffractometer with a  $\text{Cu } K\alpha$  radiation ( $\lambda = 0.15418 \text{ nm}$ ) and a graphite monochromator. FTIR spectra of the samples were recorded on a Nicolet 5DX-FTIR spectrometer using the KBr pellet method in the range of 400—4000  $\text{cm}^{-1}$ . The morphology and microstructure of the samples were characterized using a scanning electron microscope (SEM, Hitachi S4800). The mechanical properties of the membranes were characterized by a tensile tester (XG-1A). Each membrane was cut into strips, which had a width of 1.5 mm and a length of 1.5 cm. Then long membrane strips were sandwiched vertically on the tensile tester, and stretched in the length direction with a stretching velocity of 1 mm/min.

## 2 Results and Discussion

In this experiment,  $\text{AlCl}_3 \cdot 6\text{H}_2\text{O}$  and AIP were used as the aluminum source. Water was added as the solvent. Ethyl alcohol was used as an assistant solvent to accelerate solvent volatilization during the electrospinning process and benefit the fibers' drying and rapid gelation. After dissolution in water,  $\text{AlCl}_3 \cdot 6\text{H}_2\text{O}$  was in the form of  $[\text{Al}(\text{H}_2\text{O})_6]^{3+}$ . Tartaric acid was added as a spinning additive to react with  $\text{Al}(\text{III})$  to form carboxylic acid aluminum, which further formed intermolecular bonds and a complex carboxyl aluminum network. The formation of carboxyl aluminum network increased the viscosity of the sol and improved its spinnability. Concentrated hydrochloric acid was added to adjust the pH value of the solution to 2 and promote the hydrolysis of aluminum isopropoxide into amorphous  $\text{AlO}(\text{OH})$  colloidal particles<sup>[17,18]</sup>. The colloidal particles were positively charged according to the *zeta* potential analyzer test. TEM image of colloidal particles (Fig.1) shows that the size of the colloidal particles was about 5 nm, and the small size resulted in obtaining fibers composed of small grains. PVP was used as the spinning additive to improve the spinnability of the precursor. Spherical colloidal particles were uniformly dispersed and stable in the sol due to the addition of PVP. Also, the sol was more easily stretched into one-dimensional fibers by the electric force due to the linear structure of PVP. The sol was suitable for forming fibrous membranes in the viscosity range from 0.058 to 0.065  $\text{Pa} \cdot \text{s}$ , and the viscosity of sol could be controlled by adjusting the amount of PVP.

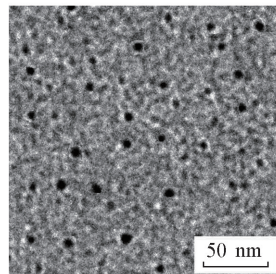


Fig.1 TEM image of the colloidal particles

The proportion of aluminum chloride and aluminum isopropoxide, and the added amount of PVP have significant effects on the morphology of the final products with this method. Products in membrane form could be obtained when the molar ratio of aluminum chloride and aluminum isopropoxide was in the range from 1 : 2.5 to 1 : 0.67. The gel fibrous membrane was complete and uniform as shown in Fig.2 (A), and there were no holes, cracks or other obvious defects in the membrane. Fig.2 (B) shows that the gel fibrous membranes are composed of overlapped fibers, and the thickness of the fibrous membranes was homogeneous. No obvious defects could be observed by an optical microscope. The molar ratio of aluminum chloride to

aluminum isopropoxide significantly affects the spinnability of the sol. The products obtained *via* this method were not in membranous form but in cotton-shaped form when the molar ratio of aluminum chloride to aluminum isopropoxide was less than 1 : 2.5. When the molar ratio of aluminum chloride to aluminum isopropoxide was greater than 1 : 0.67, the sol did not have spinnability. Different proportions of aluminum sources resulted in various contents of colloidal particles and ions in the sol, as well as various electrical conductivities. Fibers have different modes of motion in high voltage electrostatic fields, what inevitably lead to products of various morphologies. The membrane could be formed when the added amount of PVP was in the range from 1.2% to 1.8% (mass fraction) of the solution. When the PVP amount was smaller than 1.2% (mass fraction), the viscosity of the sol was so small that the sol had no spinnability. Conversely, when excessive PVP of more than 1.8% (mass fraction) was added, a cotton-shaped product was easily obtained. When the PVP amount was in the range from 1.4% to 1.6% (mass fraction), the fibrous membrane prepared *via* this method was uniform and had a large surface area.

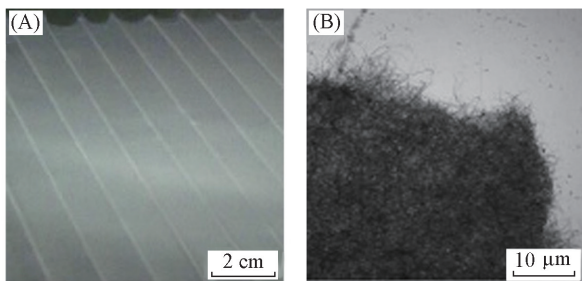


Fig.2 Optical image(A) and optical microscope image(B) of gel fibrous membrane

TG-DSC curves of the fibrous membrane are shown in Fig. 3(A). It can be seen from the TG curve that there were two substantial mass losses from room temperature to 600 °C with a total loss of *ca.* 61.77%. The first mass loss below 350 °C was attributed to the decomposition of tartaric acid<sup>[19]</sup> and departure of water, ethanol and isopropanol<sup>[19,20]</sup>. The mass loss from 350 to 600 °C was attributed to the decomposition of PVP. There were two obvious exothermic peaks in DSC curve. The first peak at 395 °C was due to the decomposition of PVP. The second one at 880 °C was due to the formation of the  $\gamma$ -Al<sub>2</sub>O<sub>3</sub> phase<sup>[21]</sup>.

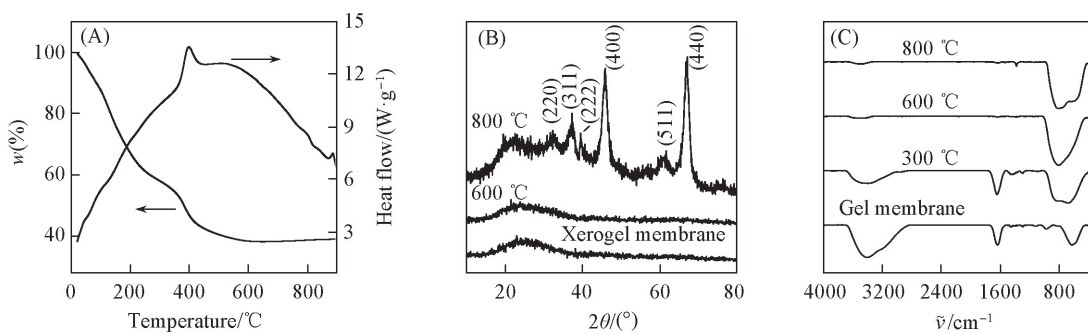


Fig.3 TG-DSC curves of the gel fibrous membrane(A), XRD patterns(B) and IR spectra(C) of different membranes

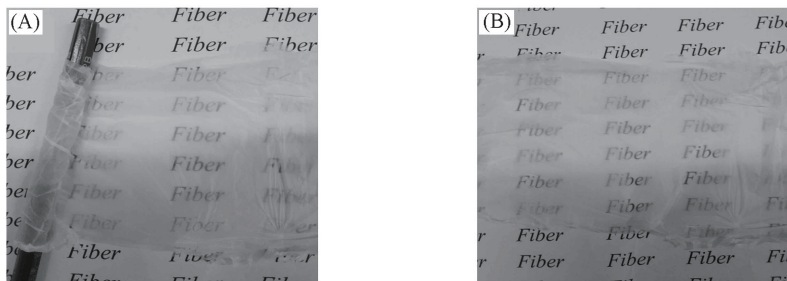
XRD analysis was used to confirm the structure of the membranes. The fibrous membranes were calcined at 600 and 800 °C to remove solvents and organics and form  $\gamma$ -Al<sub>2</sub>O<sub>3</sub> membranes. Fig.3(B) shows that the membranes without calcination and calcined at 600 °C were both amorphous. After being calcined at 800 °C for 1.5 h, obvious reflections of  $\gamma$ -Al<sub>2</sub>O<sub>3</sub> (JCPDS No. 50-0741) (220), (311), (222), (400), (511) and (440) indicated that high-crystallinity  $\gamma$ -Al<sub>2</sub>O<sub>3</sub> fibrous membranes were formed. The wide shape of the diffraction peaks indicated that the fibers had a smaller crystalline size. That  $\gamma$ -Al<sub>2</sub>O<sub>3</sub> formed at 800 °C but not 880 °C as the DSC curve showed was due to the slower heating rate of the actual calcination than that of the DSC test. On the other hand, in the phase transition process from amorphous alumina to  $\gamma$ -Al<sub>2</sub>O<sub>3</sub>, the rearrangement and ordering of atoms were relatively slow.

Fig.3(C) shows the IR spectra of the gel fibrous membranes and those calcined at different temperatures for 1.5 h. The broad bands around 3420 cm<sup>-1</sup> indicated the stretching vibration of hydroxyls in water, ethanol

and tartaric acid. The absorptions around  $1644\text{ cm}^{-1}$  was attributed to the bending vibration of hydroxyls and the vibration of carbonyl in PVP<sup>[21,22]</sup>, and those around  $630$ ,  $690$  and  $820\text{ cm}^{-1}$  were assigned to the vibration of  $\text{AlO}_6$  and  $\text{AlO}_4$ , respectively. The absorptions from  $900$  to  $1200\text{ cm}^{-1}$  were due to the vibration of  $\text{Al—OH}$ <sup>[23]</sup>. The shoulder peak at  $2970\text{ cm}^{-1}$ , and the peaks observed from  $1200$  to  $1500\text{ cm}^{-1}$  were attributed to the characteristic vibrations of PVP<sup>[21]</sup>. When the fibrous membrane was calcined at  $300\text{ }^\circ\text{C}$ , the absorptions around  $3420$  and  $1644\text{ cm}^{-1}$  obviously decreased, confirming the removal of water, ethanol and tartaric acid. After calcinations at  $600\text{ }^\circ\text{C}$ , the characteristic peaks of PVP almost disappeared due to the decomposition of the polymer.

The as-prepared membranes had excellent flexibility. The membranes shrank when they were dried and calcined at different temperatures. The membranes were cut into rectangles to study the shrinkage of the membranes during the calcination process. The side length shrinking percentage of the membranes dried at  $70\text{ }^\circ\text{C}$ , and calcined at  $300$ ,  $600$  and  $800\text{ }^\circ\text{C}$  were  $11.1\%$ ,  $35.6\%$ ,  $37.1\%$  and  $41.8\%$  respectively. The shrinkage mainly occurred before  $300\text{ }^\circ\text{C}$ , and was caused by the departure of ethanol, water and organics. Although PVP decomposed from  $300$  to  $600\text{ }^\circ\text{C}$ , due to the small addition amount of PVP, the shrinkage of the fibrous membranes was not obvious. From  $600$  to  $800\text{ }^\circ\text{C}$ , the fibrous membranes had a slight shrinkage, which was attributed to the disordered Al and O atoms in fibers tending to build up a long-range order structure during the process of *gamma* phase transition from amorphous alumina. The membranous form and the flexibility of the membranes were retained during the calcination process.

The flexibility of the nanofibrous membranes could be qualitatively and intuitively demonstrated by bending the membranes around a pencil [ Fig.4(A) ]. Fig.4(B) shows that the membranes after twining round a pencil could recover their original shape, without any cracks appearing during the process. This excellent flexibility can further expand the application field of inorganic fibrous membranes.



**Fig.4 Optical images of the  $\gamma$ - $\text{Al}_2\text{O}_3$  fibrous membranes**

(A) Bending around a pencil; (B) after twining around the pencil.

Fig.5 presents the representative SEM images and corresponding fiber diameter distribution of the  $\gamma$ - $\text{Al}_2\text{O}_3$  membranes. Fig.5(A) indicates that the membranes were complete and uniform, the fibers' orientation was random, and there were no defects such as cracks or big holes in the membranes. Membranes without defects are inclined to have higher strength. There were almost no broken fibers in Fig.5(A), which qualitatively demonstrates that the fibrous membranes have good strength and would not be easily damaged in actual use. Fig.5(B) presents the membrane's cross section, and the thickness was about  $25\text{ }\mu\text{m}$ . With the prolongation of electrospinning time, the membrane gradually thickened. The fibrous membranes prepared *via* this method presented a uniform and fine fiber diameter [ Fig.5(C) ]. The fibers composing the membranes were independent, without inter-fibrous junctions, which gives the membranes excellent flexibility<sup>[16]</sup>. Fig.5(D) indicates that the fibers' surface was smooth, and there were no apparent pores in the fibers. The fracture surface of the fibers revealed that the fibers were composed of nanoparticles ranging from  $15$  to  $30\text{ nm}$  [ Fig.5(E) ]. The small size of the grain is good for high fiber strength and indirectly improves the strength of the fibrous membranes<sup>[24]</sup>. The membranes had a narrow diameter distribution with most fibers' diameter

distributed in the range from 140 nm to 240 nm. The mean diameter was about 188 nm [ Fig.5(F) ].

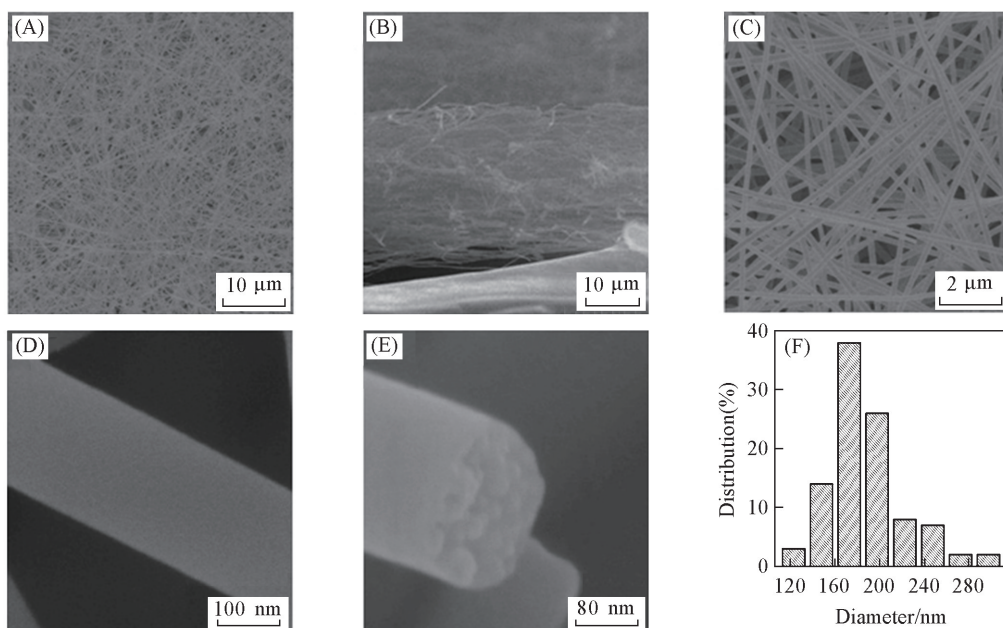


**Fig.5 SEM images of  $\gamma$ - $\text{Al}_2\text{O}_3$  fibrous membranes(A—E) and the diameter distribution of the membrane(F)**

(A), (C) Surface of the membrane; (B) cross section of the membrane; (D) single fiber's surface of the membrane; (E) fracture section of a fiber of the membrane.

The tensile strength of the membranes was studied by a tensile tester. The membranes were cut into strips (1.5 cm $\times$ 1.5 mm). The membranes' tensile strength (MPa) can be calculated by the following formula:

$$\text{Tensile strength} = \frac{\text{Breaking force}}{\text{Width} \times \text{Thickness}}$$

where the units of breaking force, width and thickness are cN, cm and  $\mu\text{m}$ , respectively.

Fig.6 presents the membranes' strength-strain curves. All the curves can be divided into two stages by the highest strength point. In the first stage, the strength increased with the increase of the strain, and the fibers' arrangements in the membranes changed from unordered to well-organized by the fibers' dislocation and slipping. The strength in the stage was mainly contributed by the sliding friction force between fibers, and secondarily caused by the strength of the fibers themselves. At the highest strength point, the fibers can not resist the tensile force and begin to fracture. The curves then enter the second stage. In this stage, the strength decreased with the increase of the strain. During the process, the ordered fibers slid in the fiber-direction and gradually fractured. The strength in the second stage was mainly caused by the sliding friction force and the strength of fibers. The fracture processes of the membranes are similar to the report of Mao *et al.*<sup>[7]</sup>.

The strength of the xerogel fibrous membrane was 0.14 MPa. For the membranes calcined at 300, 600, 700 and 800  $^{\circ}\text{C}$ , the strength were 0.50, 1.24, 1.26 and 1.01 MPa, respectively (Fig.6). It can be seen from the data that the strength first increases and the interacting forces among the particles were weak, so the strength of the xerogel nanofibrous membrane was very low. By calcinating, the fibrous membranes significantly shrank with the removal of the ethanol, water and organics. The fibers combined more tightly, and

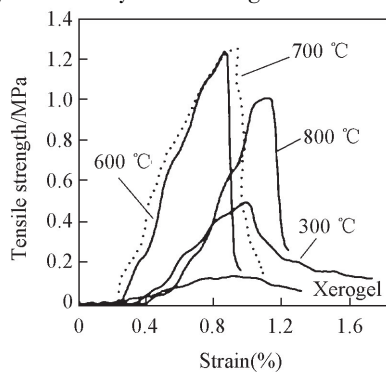


**Fig.6 Tensile strength-strain curves of the xerogel membranes and those calcined at different temperatures**

the interacting force among the particles in the fibers became higher, so the sliding friction force and the fiber strength increased, which resulted in an increase in the membrane's strength. The  $\gamma$ -Al<sub>2</sub>O<sub>3</sub> membranes formed after calcination at 800 °C. The fiber strength became lower due to the particles' growth and the formation of pores, which resulted in a decrease of the membrane's strength.

### 3 Conclusions

High-strength flexible  $\gamma$ -Al<sub>2</sub>O<sub>3</sub> membranes were fabricated by electrospinning combined with sol-gel technique. The membranes' morphology, the fibers' arrangement and the crystalline phase have an important impact on the flexibility and mechanical properties of the membranes. The  $\gamma$ -Al<sub>2</sub>O<sub>3</sub> membranes present excellent flexibility and tensile strength (1.01 MPa). The excellent flexibility and high tensile strength may extend the membrane's service life. The membranes prepared by this method will have a lot of potential applications in catalytic and high-temperature filtration fields.

*Thanks to Dr. Edward C. Mignot, Shandong University, for linguistic advice.*

This paper is supported by the Innovation Project of Shandong Academy of Medical Sciences, the National Natural Science Foundation of China (No. 21305079) and the Natural Science Foundation of Shandong Province, China (No. ZR2015YL040).

### References

- [ 1 ] Hu F., Wang Y., Lai X., Wu Y., Du F., Wang C., *Chem. Res. Chinese Universities*, **2015**, 31(1), 156—159
- [ 2 ] Zhang P., Chen D., Jiao X., *Eur. J. Inorg. Chem.*, **2012**, 2012(26), 4167—4173
- [ 3 ] Zhang P., Jiao X., Chen D., *Mater Lett.*, **2013**, 91(3), 23—26
- [ 4 ] Su V., Terehov M., Clyne B., *Adv. Eng. Mater.*, **2012**, 14(12), 1088—1096
- [ 5 ] Mahapatra A., Mishra B. G., Hota G., *Ind. Eng. Chem. Res.*, **2012**, 52(4), 1554—1561
- [ 6 ] Guan J., Li J., Li Y., *RSC Adv.*, **2016**, 6(40), 33781—33788
- [ 7 ] Zhang P., Lu W., Wang Y., Jiao X., Chen D., *J. Sol-gel Sci. Techn.*, **2016**, 8(3), 690—696
- [ 8 ] Chen L. M., Cao J., Ye L., Zhang A. Y., Feng Z. G., *Chem. J. Chinese Universities*, **2016**, 37(3), 600—606
- [ 9 ] Ge J., Si Y., Fu F., Wang J., Yang J., Cui L., Ding B., Yu J., Sun G., *RSC Adv.*, **2013**, 3(7), 2248—2255
- [ 10 ] Clark J. E., Olesik S. V., *Anal. Chem.*, **2009**, 81(10), 4121—4129
- [ 11 ] Park S. J., Chase G., Jeong K. U., Kim H., *J. Sol-gel Sci. Techn.*, **2010**, 54(2), 188—194
- [ 12 ] Biswas A., Park H., Sigmund W. M., *Ceram. Int.*, **2012**, 38(1), 883—886
- [ 13 ] Tan E. P. S., Lim C. T., *Appl. Phys. Lett.*, **2004**, 84(9), 1603—1605
- [ 14 ] Yang L., Fittie C. F. C., Werf K. O. V. D., Bennink M. L., Dijkstra P. J., Feijen J., *Biomaterials*, **2008**, 29(8), 955—962
- [ 15 ] Wang N., Raza A., Si Y., Yu J., Sun G., Ding B., *J. Colloid Interf. Sci.*, **2013**, 398, 240—246
- [ 16 ] Li L., Hashaikheh R., Arafat H. A., *J. Membrane Sci.*, **2013**, 436, 57—67
- [ 17 ] Huang Y. L., Xue D. S., Zhou P. H., Ma Y., Li F. S., *Mater. Sci. Eng. A*, **2003**, 359(1/2), 332—337
- [ 18 ] Yoldas B. E., *J. Am. Ceram. Soc.*, **1982**, 65(8), 387—393
- [ 19 ] Yalcin D., Ozealik O., Altioek E., Bayraktar O., *J. Therm. Anal. Calorim.*, **2008**, 94(3), 767—771
- [ 20 ] Nuansing W., Ninmuang S., Jarernboon W., Maensiri S., Seraphin S., *Mater. Sci. Eng. B*, **2006**, 131(1—3), 147—155
- [ 21 ] Mahapatra A., Mishra B. G., Hota G., *Ceram. Int.*, **2011**, 37(7), 2329—2333
- [ 22 ] Chen X., Gu L., *J. Sol-gel Sci. Techn.*, **2008**, 46(1), 23—32
- [ 23 ] Chandradass J., Balasubramanian M., *J. Mater. Process. Tech.*, **2006**, 173(3), 275—280
- [ 24 ] Tan E. P. S., Lim C. T., *Appl. Phys. Lett.*, **2004**, 84(9), 1603—1605

(Ed.: F, K, M)